# Hybrid Human-in-The-Loop Simulations for Evaluating Detect and Avoid System

1st Jung-Hwan Park

dept. of Aerospace Engineering and
the Program in Aerospace Systems Convergence
Inha University
Incheon, Republic of Korea
jh-park@inha.edu

3<sup>rd</sup> Jaeyoung Ryu

dept. of Aerospace Engineering and the Program in Aerospace Systems Convergence Inha University Incheon, Republic of Korea JaeyoungRyu@inha.edu 2<sup>nd</sup> Tae Young Kim

dept. of Aerospace Engineering and
the Program in Aerospace Systems Convergence
Inha University
Incheon, Republic of Korea
taeyoungkim@inha.edu

4<sup>th</sup> Hak-Tae Lee

dept. of Aerospace Engineering and
the Program in Aerospace Systems Convergence
Inha University
Incheon, Republic of Korea
haktae.lee@inha.ac.kr

Abstract-Detect And Avoid (DAA) is one of the most important functionalities for the operation of large Unmanned Aircraft Systems (UAS). Since the UAS pilot must maneuver the aircraft by interacting with the DAA system and Air Traffic Control (ATC), studying their interactions is essential for the further development of such systems. However, conducting flight tests requires high-performance UASs and large airspaces. In contrast, flight testing with smaller surrogate UASs is logistically easier but integration with the ATC is difficult because they tend to fly at lower altitudes and are not detected by the standard radar surveillance systems. This study proposes alternative testing methods based on smaller surrogate UAS. First, the DAA system parameters are scaled based on the speeds of the surrogate UASs so that the time scale remains the same. Second, compact standalone Automatic Dependent Surveillance - Broadcast (ADS-B) out transponders are installed on the surrogate UASs so that the surveillance information is received by ADS-B receivers. Two phase flight tests were conducted. The first tests were with a simulated virtual intruder with an ADS-B out equipped drone. The second test involved two drones, each equipped with an ADS-B out transponders The escalation in alert levels and the execution of avoidance maneuvers according to the ATC instructions were successfully executed. Both tests demonstrated that it is possible to conduct DAA flight tests using surrogate UAS that are realistic enough to mimic the larger system, and it can become a cost-effective tool for studying the interactions between UAS pilots, the DAA system, and ATC.

Index Terms—Detect and Avoid, Human-in-The Loop Simulations, ADS-B, DAIDALUS

## I. INTRODUCTION

UASs have proven their strategic importance in military contexts, such as in the war in Ukraine, where their stealth

This work was supported grant RS-2025-04322968 funded by the Ministry of Land, Infrastructure and Transport and by grant RS-2021-KT216489 funded by Korea AeroSpace Administration of the Korean government.

capabilities and operational flexibility attracted global attention [1]. In the civil sector, the trend of Advanced Air Mobility is gaining significant momentum. As UASs begin to share airspace with manned aircraft, ensuring safe and reliable separation becomes critical. As a result, the development and certification of Detect and Avoid (DAA) systems have become a critical challenge [2], [3].

The Radio Technical Commission for Aeronautics (RTCA) has established the DO-365 Minimum Operational Performance Standards (MOPS) [4], which define the operational and technical criteria for DAA systems.

One of the earliest large-scale DAA flight tests was conducted by Northrop Grumman in 2007 using manned aircraft such as the Beechcraft King Air and Learjet Model 25B. The test used a combination of Electro-Optical/Infrared (EO/IR) sensors, radar, Traffic Collision Avoidance System, ADS-B, and Traffic Information Service – Broadcast for detection and used the Passive Ranging and Collision Avoidance algorithm [5].

In Europe, 2010, the Mid-air Collision Avoidance System (MIDCAS) project conducted a series of DAA flight tests using manned aircraft such as the CASA C-212, Falcon-Mystere 20, and PC-7 turboprop, alongside the Sky-Y UAS [6]. The sensor suite included EO/IR, radar, transponder interrogator, and ADS-B. In 2015, NASA conducted a DAA flight test at its flight research center in California, involving an MQ-9 UAS and a Cessna 172 aircraft [7]. ADS-B In/Out was used as the primary sensing mechanism.

Flight tests have been conducted with small UAS using vision-based detection techniques [8], [9], while numerous DAA human-in-the-loop (HiTL) simulations using pseudopilots have been studied. [10]–[14].

This study proposes a hybrid HiTL simulation framework

combined with scaled flight tests using small surrogate UAS equipped with ADS-B out transceivers. A DAA parameter scaling method is presented to preserve temporal equivalence during encounters by reducing the spatial parameters according to the surrogate UAS speeds. A fully functional ATC simulation environment is integrated with live ADS-B data from actual drones and virtual aircraft by pseudo-pilots. Two flight tests were conducted to demonstrate the feasibility of the proposed approach: one with a virtual aircraft and a drone with ADS-B out, the other with two drones with ADS-B out executing scaled encounter scenarios.

Following this Introduction, Section II introduces a DAA algorithm scaling methodology for slower surrogate UASs. Section III describes the system setup for flight tests including the regulatory procedures for ADS-B out in the Republic of Korea. Section IV presents the design and execution of two flight tests. Finally, Section V summarizes the results, discusses the implications for scaled DAA validation, and outlines directions for future research.

## II. DAA WELL CLEAR SCALING

This section introduces the scaling technique used to enable the slower surrogate UAS. The core idea is that timings can be preserved if the distance and the speed are scaled by the same factor.

## A. DAA Well Clear Definition

DAA Well Clear (DWC) boundaries consist of horizontal modified tau, Horizontal Miss Distance (HMD), and vertical separation. Modified tau,  $\tau_{mod}$ , is the time remaining until the horizontal distance between the two aircraft is at its minimum from the current time assuming both the aircraft maintain constant velocity at the current time step, and this minimum value is HMD. Loss of Well Clear (LoWC) is defined when all three metrics are smaller than their thresholds at the same time. Less severe alert levels are defined based on the remaining time to LoWC. A detailed description of the parameters and the mathematical formulation can be found in [4].

TABLE I: Parameters for En-Route DWC Alerts

| Alert Type         | Preventive<br>Alert | Corrective<br>Alert | Warning<br>Alert | LoWC     |
|--------------------|---------------------|---------------------|------------------|----------|
| Average Alert Time | 55 sec              | 55 sec              | 25 sec           | 0 sec    |
| $	au_{mod}^*$      | 35 sec              | 35 sec              | 35 sec           | 35 sec   |
| $DMOD, HMD^*$      | 4,000 ft            | 4,000 ft            | 4,000 ft         | 4,000 ft |
| $d_h^*$            | 700 ft              | 450 ft              | 450 ft           | 450 ft   |

# B. DAA Well Clear Parameter Scaling

In the DAA formulations, when a distance parameter is scaled by a factor k, the scaled distance  $\hat{d}$  can be expressed as shown in Eq. (1).

$$\hat{d} = kd \tag{1}$$

If time is not scaled, the scaled velocity,  $\hat{v}$ , is scaled by the same factor k as in Eq. (2)

$$\hat{v} = \frac{d}{dt} \left( \hat{d} \right) = \frac{d}{dt} \left( kd \right) = kv \tag{2}$$

If the scaled DMOD parameter is denoted by  $D\hat{M}OD$ , scaled  $\tau_{mod}$ , denoted by  $\hat{\tau}_{mod}$  can be expressed as in Eq. (3).

$$\hat{\tau}_{mod} = \frac{D\hat{M}OD^{2} - \hat{r}_{xy}^{2}}{\hat{d}_{x}\hat{v}_{rx} + \hat{d}_{y}\hat{v}_{ry}} 
= \frac{k^{2} \left(\frac{D\hat{M}OD}{k}\right)^{2} - k^{2}r_{xy}^{2}}{kd_{x} \cdot kv_{rx} + kd_{y} \cdot kv_{ry}} 
= \frac{\left(\frac{D\hat{M}OD}{k}\right)^{2} - r_{xy}^{2}}{d_{x} \cdot v_{rx} + d_{y} \cdot v_{ry}} = \tau_{mod}$$
(3)

For the scaled  $\hat{\tau}_{mod}$  to be the same as the original  $\tau_{mod}$ , DMOD must be scaled by the same factor k as in Eq. (4).

$$D\hat{M}OD = k \cdot DMOD \tag{4}$$

As shown in Eq. (3),  $\tau_{\rm mod}$  consists only of temporal dimensions and thus remains unaffected by the scaling of spatial dimensions. Therefore, by reducing one of the DWC boundaries, specifically DMOD, in proportion to the ratio between the simulated speed and the actual flight speed, the alert can be triggered at the same time as in full-scale operations.

The scaled time to the horizontal closest point of approach,  $\hat{t}_{CPA}$ , is not changed by distance scaling as shown in Eq. (5).

$$\hat{t}_{CPA} = -\frac{\hat{d}_x \hat{v}_{rx} + \hat{d}_y \hat{v}_{ry}}{\hat{v}_{rx}^2 + \hat{v}_{ry}^2}$$

$$= -\frac{(kd_x)(kv_{rx}) + (kd_y)(kv_{ry})}{(kv_{rx})^2 + (kv_{ry})^2}$$

$$= -\frac{d_x v_{rx} + d_y v_{ry}}{v_{rx}^2 + v_{ry}^2} = t_{CPA}$$
(5)

Using the  $t_{CPA}$ , which is not affected by scaling, it is shown that the HMD also scales by the same factor k as in Eqs. (6) through (8)

$$\hat{D}_x = \hat{d}_x + \hat{v}_{rx}\hat{t}_{CPA} = kd_x + kv_{rx}t_{CPA} = kD_x$$
 (6)

$$\hat{D}_{y} = \hat{d}_{y} + \hat{v}_{ry}\hat{t}_{CPA} = kd_{y} + kv_{ry}t_{CPA} = kD_{y}$$
 (7)

$$H\hat{M}D = \sqrt{\hat{D}_x^2 + \hat{D}_y^2} = k\sqrt{D_x^2 + D_y^2} = kHMD$$
 (8)

For vertical separation, the altitudes and altitude thresholds scaled by any factor are equivalent to the original formulation as given in Eq. (9).

$$kh_2 - kh_1 < kd_h^* \tag{9}$$

# C. Detect and AvoID Alerting Logic for Unmanned Systems (DAIDALUS)

DAIDALUS, developed by NASA, supports the safe integration of high-performance unmanned aircraft into civil airspace [15]. The system is designed to operate over a wide range of airspeeds, from a minimum of 40 knots to a maximum of 600 knots, in accordance with the operational performance and altitude specifications for unmanned aircraft as defined in RTCA DO-365A. The DAIDALUS algorithm provides conflict resolution advisories by issuing one of four maneuver types, enabling UAS pilots to effectively manage potential encounter scenarios.

The DAIDALUS algorithm includes a configuration file in which the DWC threshold values are specified. While this file also contains parameters required to generate appropriate maneuver suggestions, the present study focuses only on the alerting functionality, leaving the maneuver decision-making to the air traffic controllers. To enable scaled-down testing, the spatial threshold values,  $HMD^*$ ,  $DMOD^*$ , and  $d_h^*$ , are reduced according to the scale factor, k.

Distance scaling has been validated through half-scale fast-time simulations using DAIDALUS. Two encounter scenarios are tested: head-on course and converging at a 60 degree angle. Both scenarios occur at the same altitude, with no vertical maneuvers. In the initial unscaled simulation, both the aircraft fly at 100 knots. For the 50% scaled cases, the parameters in Table II are used with both the aircraft flying at 50 knots. As can be seen in Fig. 1, the timings of the Corrective Alert, the Warning Alert, and the LoWC were exactly the same.

This result suggests that even when using slower surrogate aircraft, it is possible to provide both pilots and controllers with the same simulation experience as would be observed in full-speed flight.

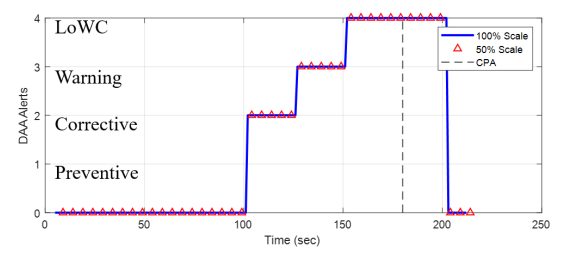
TABLE II: Parameters for scaled En-Route DWC Alerts (k = 0.5)

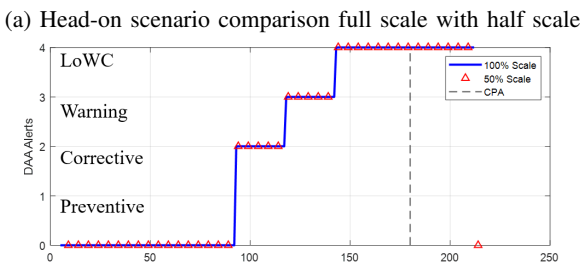
| Alert Type      | Preventive<br>Alert | Corrective<br>Alert | Warning<br>Alert | LoWC     |
|-----------------|---------------------|---------------------|------------------|----------|
| Avg. Alert Time | 55 sec              | 55 sec              | 25 sec           | 0 sec    |
| $	au^*_{mod}$   | 35 sec              | 35 sec              | 35 sec           | 35 sec   |
| $DMOD, HMD^*$   | 2,000 ft            | 2,000 ft            | 2,000 ft         | 2,000 ft |
| $d_h^*$         | 350 ft              | 225 ft              | 225 ft           | 225 ft   |

#### III. TEST PREPARATION

## A. Authorization Process for ADS-B Out

Long regulatory processes involving multiple government agencies are required to use the ADS-B out in the Republic of Korea. If the mass of the UAS exceeds 2 kg, or is used commercially, the UAS must be registered with the Korea Transportation Safety Authority. Once the UAS is registered, an application for ICAO address allocation is submitted to the Air Navigation Satellite Policy Division of the Ministry





(b) Converge 60° scenario comparison full scale with half scale

Fig. 1: DAIDALUS time compare with full scale and half scale

of Land, Infrastructure and Transport. Meanwhile, the ADS-B transceiver requires a radio station license and inspection, which are handled by the Ministry of Science and ICT. The processes summarized in Fig. 2 took about ten months in total for three transceivers. In particular, the inspection process requires technical knowledge and specific equipment to correctly measure the spectrum of the transceiver. These procedures are described in detail in [16].

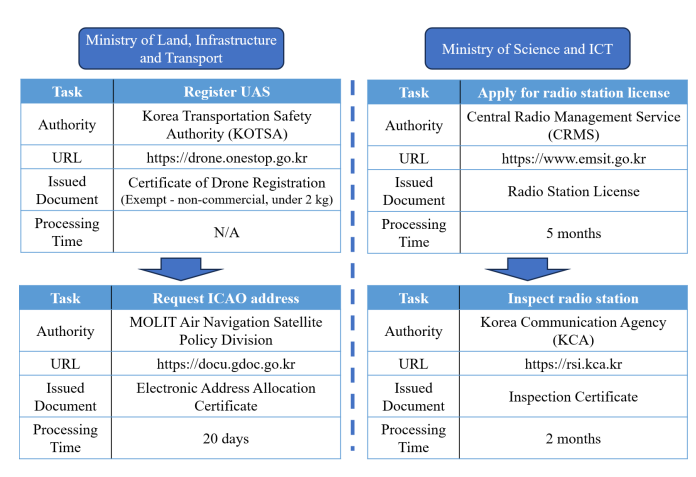


Fig. 2: Summary of required regulatory procedures to use ADS-B out

For the purposes of this study, weight was a key consideration and the Aerobits TR-1A was selected as it weighs only 14 grams. The specifications of the ADS-B out transceiver are summarized in Table III. Although the device is not certified under TSO and therefore not approved for installation on manned aircraft, its lightweight design and integrated Global Navigation Satellite Systems and barometric sensors made it suitable for installation on small surrogate UAS such as quadrotor drones.

TABLE III: ADS-B transceiver specification

| Pictures   | Spec            | Description     |  |
|--|-----------------|-----------------|--|
| TR-1A  - CHISS  - CHI | Model           | TR-1A           |  |
|  | Manufacturer    | Aerobits        |  |
|  | Country         | Poland          |  |
|  | Frequency       | 1,090 MHz       |  |
|  | Sensors         | GNSS, barometer |  |
|  | RF output power | 0.25/0.5/1 W    |  |
|  | Weight          | 14 g            |  |
|  | Input power     | 5 V             |  |

#### B. The range test of ADS-B out using surrogate UAS



Fig. 3: TR-1A ADS-B transceiver installed on a DJI Mavic Pro drone

To verify the performance of the ADS-B out transceiver after obtaining approval, a reception range test was conducted. For this test, the TR-1A transceiver was mounted on a DJI Mavic Pro drone. A custom mount was fabricated that houses a separate battery and two antennas, as shown in Fig. 3. The drone was launched from a location 6.5 km from the ADS-B receiver located at Inha University and flown farther away from the receiver. Initial signal loss observed at a distance of 8.1 km, as shown in Fig. 4. On return to the launch site, the reception was recovered when the distance was within 8.1 km. However, intermittent signal loss was detected between 7.6 km and 8.1 km as shown in Fig. 5. From this test, a reliable reception range was determined to be 7.6 km. The test was conducted at an altitude of 150 m. Direct line of sight to the receiver was confirmed using the drone's on-board camera.

#### IV. TEST RESULTS

Two flight tests were conducted with slightly different setups. The first test was conducted with a simulated virtual aircraft and a drone with ADS-B out. The second test was conducted with two drones, each equipped with ADS-B out.



Fig. 4: ADS-B out range test

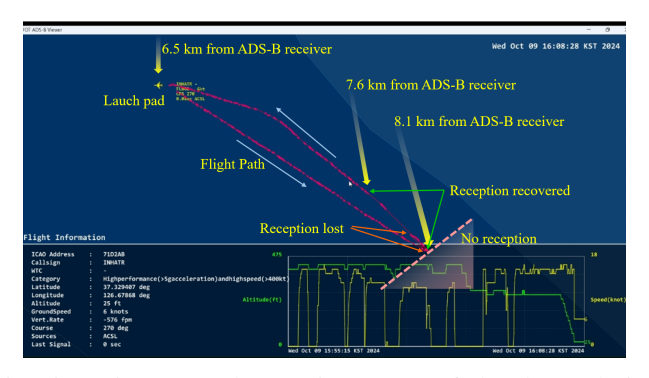


Fig. 5: Trajectory and reception status of the drone during range test

# A. Phase 1 Test - Encounter between a Virtual Aircraft and a Drone

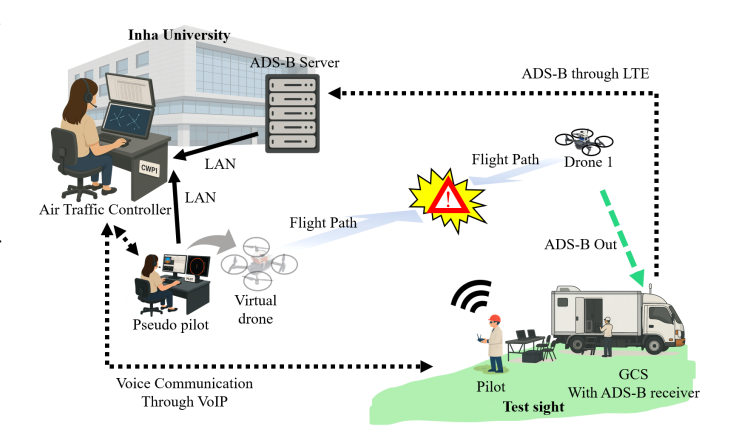


Fig. 6: Test setup for Phase 1 demonstration

The test scheme for the Phase 1 test is shown in Fig. 6. One pilot is located at Inha University's HiTL laboratory and flies a virtual aircraft created in the simulation system through the pseudo-pilot interface. The other pilot, who flies the ADS-B out equipped drone, is located at the test site. The ADS-B

signal is received by the mobile ADS-B receiver installed in the Ground Control Station (GCS) vehicle at the test site and transmitted to the HiTL laboratory through a mobile network. Both the virtual aircraft and the drone are displayed on the ATC Controller Work Position (CWP) display in the HiTL laboratory shown in Fig. 7. Voice communication between the controllers and the pilots is performed using one of the commercially available online conferencing platforms.



Fig. 7: ATC simulation facility at Inha University

Figure 8 shows the architecture of the ATC simulation system in the HiTL laboratory. Simulated aircraft are created in the pseudo-pilot modules where one pilot module can contain multiple aircraft. Each aircraft has its own DAIDALUS module, which can calculate the DWC alert levels and display blocked heading and altitude ranges for maneuver guidance as shown in Fig. 9. The simulation server combines the state information from both the simulated aircraft and real aircraft in actual flight obtained from the ADS-B receivers. It then distributes the relevant data to each simulated aircraft for the DAIDALUS module. The combined state information is also sent to the CWPs for the air traffic controllers. Each CWP contains its own DWC module which can display the alert levels in the data block.

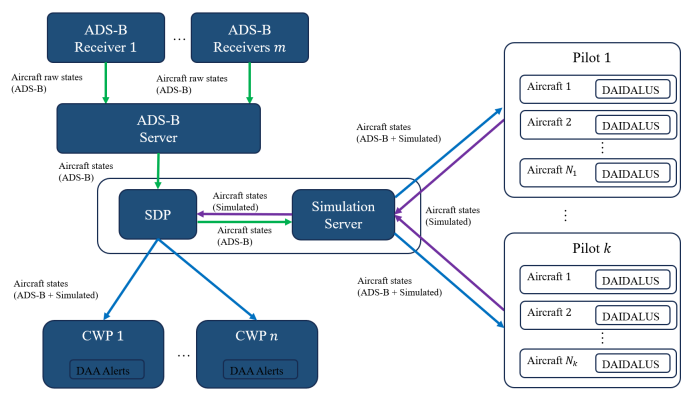


Fig. 8: ATC simulation system architecture

Phase 1 tests were conducted using the unscaled DAIDALUS algorithm. A test scenario was implemented in

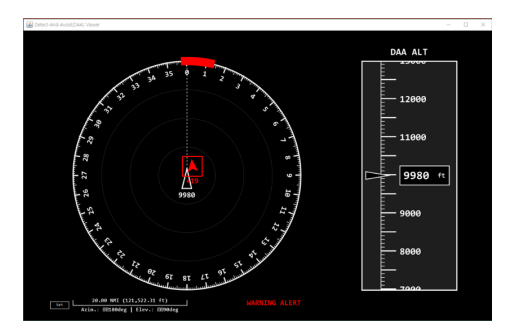


Fig. 9: DAA display in pseudo-pilot module

which a virtual UAS encountered an actual drone equipped with ADS-B out as shown in Fig. 10. A virtual UAS approached a stationary drone at a speed of 23 m/s.

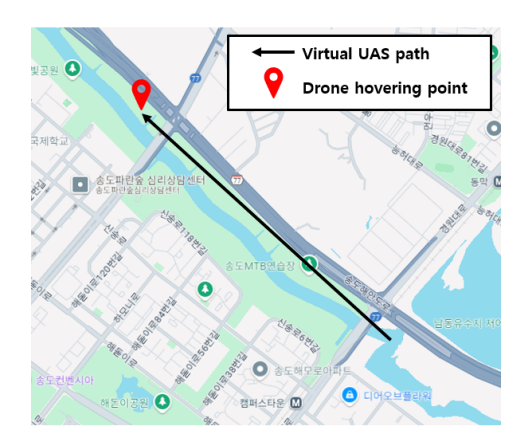
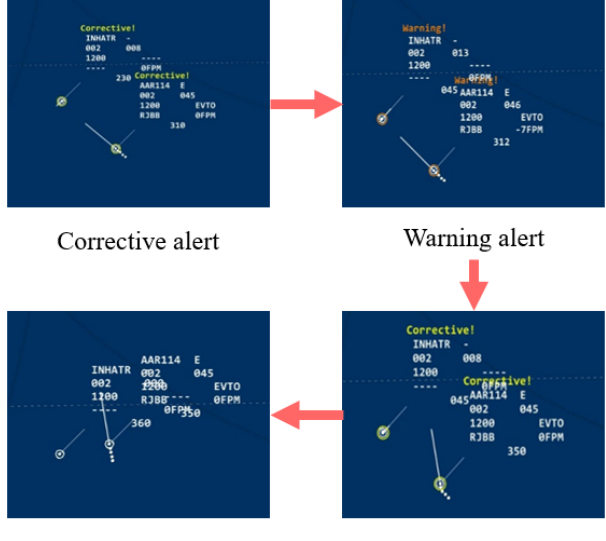


Fig. 10: Phase 1 test encounter scenario

- 1) Scenario 1 Avoidance Maneuver by the Virtual UAS: Fig. 11 illustrates the progression of targets shown in the CWP. The virtual UAS approaching the stationary drone triggered a Warning Alert, which was recognized by the air traffic controller, who subsequently issued an avoidance command to the virtual UAS pilot. The alert level then transitioned to Corrective Alert and eventually disappeared, confirming the feasibility of this type of hybrid flight test.
- 2) Scenario 2 Avoidance Maneuver by the Actual Drone: In this second scenario, the actual drone maneuvered according to the air traffic controller's instructions. Fig. 12 presents the progression of the second scenario, in which the drone starts to move towards the top right after the Corrective Alert is issued. The alert eventually escalated to Warning Alert and LoWC although the drone was at its maximum speed of 9 m/s, which means that the drone is not fast enough. This motivated the scaling of the DAA system to allow flight tests with slower surrogate air vehicles.

## B. Phase 2 Test - Encounter between Two Drones

The Phase 1 test demonstrated that all the key functionalities of the hybrid HiTL simulation system functioned as intended. In the Phase 2 experiments, the tests were conducted using a scaled DWC alert algorithm. As shown in Fig. 14, two DJI



Conflict resolved

Virtual UAS maneuvers

Fig. 11: Virtual aircraft avoid and conflict resolved

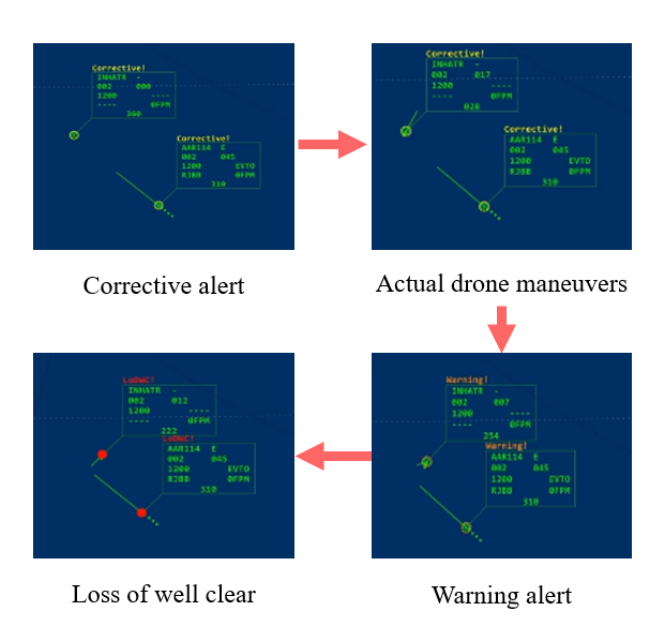


Fig. 12: Actual drone avoid and loss of well clear

Mavic Pro drones equipped with ADS-B out transceivers were used. The overall test setup is illustrated in Fig. 13, which is conceptually similar to that of Phase 1. However, no pseudopilot was used in this phase; instead, an additional ADS-B out equipped drone was used as an intruder.

In the Phase 2 test, the surrogate drones flew at about 5 m/s, which is approximately 10% of 100 knots. The scaling factor of k=0.1 was used, and all the scaled DWC parameters are listed in Table IV.

1) Scenario 0 - Verification of Scaled DWC Alerts: Scenario 0 was designed to verify the proper functionality of the scaled DWC alert logic. Two aircraft approaching head-on at a speed of 100 knots were simulated with two surrogate drones flying at 5 m/s.

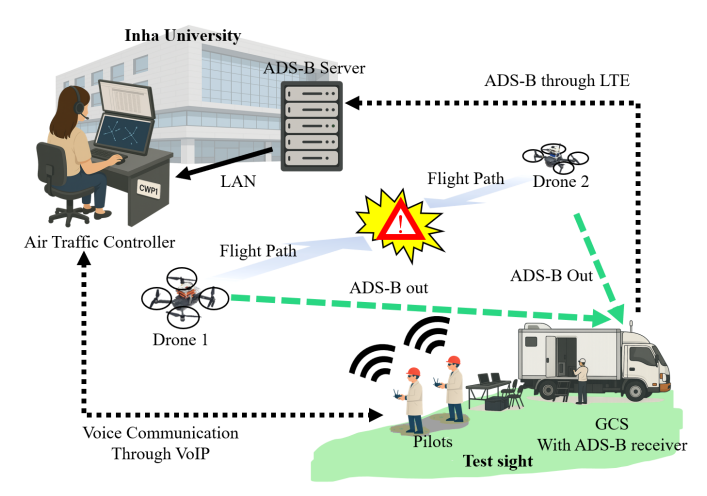


Fig. 13: Setup for Phase 2 demonstration



Fig. 14: Using 2 Drones for encounter scenario

The scenario is shown in Fig. 15, where two surrogate drones were positioned approximately 450 m away from the predicted head-on collision point, flying towards each other in opposite directions. As shown in Fig. 16, the alert sequence was triggered in the expected order. The test began with a Corrective Alert followed by a Warning Alert. Finally, the test was terminated when the LoWC was raised. It is important to note that these tests should be at the same altitude, so a Preventive Alert should not have been triggered. Intermittent Preventive Alerts were observed due to minor altitude deviations.

This scenario confirmed that the two drones, the ADS-B systems, and the GCS operated as intended. The DWC alert logic functioned correctly, and all associated communication channels remained stable throughout the test.

TABLE IV: Parameters for scaled En-Route DWC Alerts (k = 0.1)

| Alert Type         | Preventive<br>Alert | Corrective<br>Alert | Warning<br>Alert | LoWC   |
|--------------------|---------------------|---------------------|------------------|--------|
| Average Alert Time | 55 sec              | 55 sec              | 25 sec           | 0 sec  |
| $	au_{mod}^*$      | 35 sec              | 35 sec              | 35 sec           | 35 sec |
| DMOD, HMD          | 400 ft              | 400 ft              | 400 ft           | 400 ft |
| $d_h^*$            | 70 ft               | 45 ft               | 45 ft            | 45 ft  |

2) Scenario 1 - Head-on Encounter: Similar to Scenario 0, Scenario 1 involves two surrogate drones positioned approximately 450 m away from the predicted encounter point, flying



Fig. 15: Head-on encounter geometry for scenarios 0 and 1

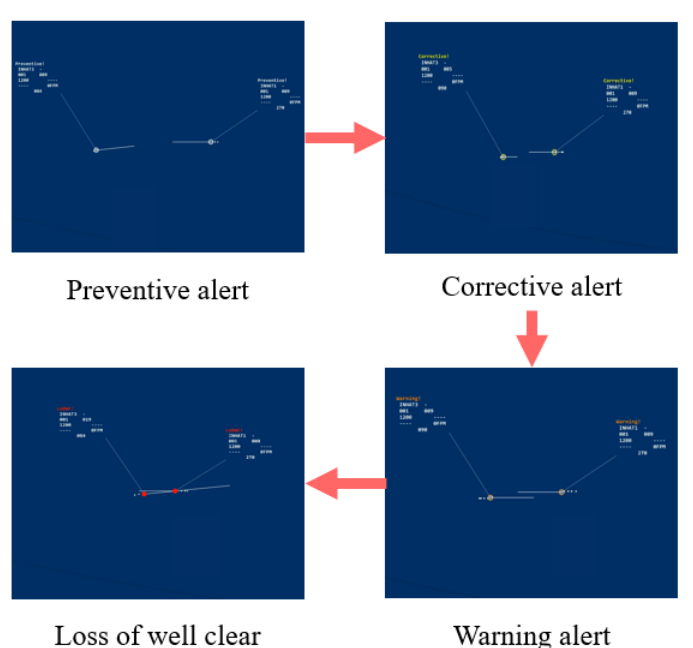


Fig. 16: Head-on scenario using Scaled DAIDALUS algorithm

towards each other from opposite directions. However, unlike the previous scenario, the controller actively intervenes upon detection of the Warning Alert.

Once the Warning Alert is issued in the CWP system and recognized by the controller, an avoidance instruction is issued to the ownship drone pilot. As shown in Fig. 17, the surrogate drone acting as the ownship positioned on the right turns 90 degrees to the right to avoid the conflict according to the controller instruction.

3) Scenario 2 - Converging at a 60 degree angle: Scenario 2 represents a converging encounter. Two surrogate drones were configured to approach the same point from directions approximately 60 degrees apart. To initiate the scenario, both drones navigated to predefined positions located approximately 450 m from the point, as shown in Fig. 18, and began approaching this point of conflict simultaneously.

As in Scenario 1, when a Warning Alert was triggered in the CWP system and recognized by the controller, an avoidance instruction was issued to resolve the conflict. As shown in Fig. 19, the ownship drone approaching from the east executed a clockwise turn to a heading of 30 degrees as an avoidance maneuver and resolved the conflict.

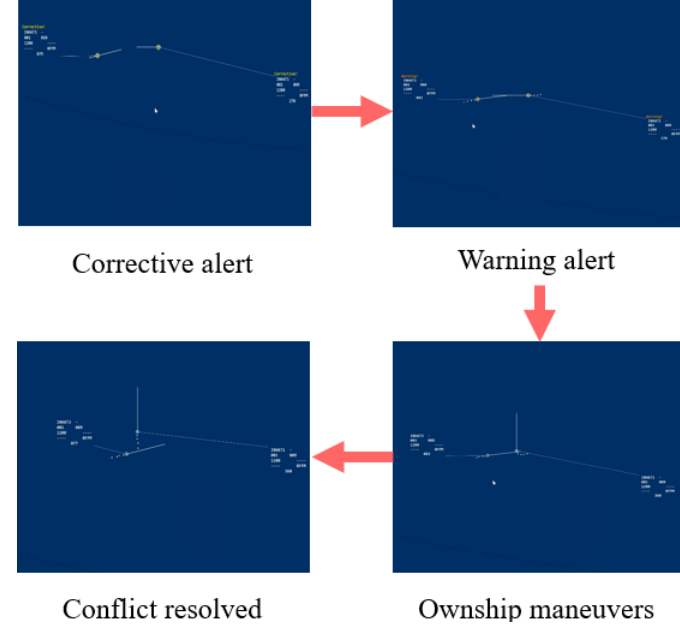


Fig. 17: UAS encounter scenario using Scaled DAIDALUS algorithm



Fig. 18: 60-degree converging encounter geometry for scenario

#### C. Discussions

Although the flight tests demonstrated most of the intended interactions, several shortcomings were identified that can be improved in future studies. First, since the altitude scaling can be independent of the horizontal distance scaling, a more appropriate scaling factor could be selected to make the altitude related alerting behavior more robust. Second, during the maneuvering of the surrogate UAS, the turn rate were greater than that of the larger UAS. Limiting selected performance parameters in the flight control system of the surrogate UAS is likely to make the system more similar to the larger UASs.

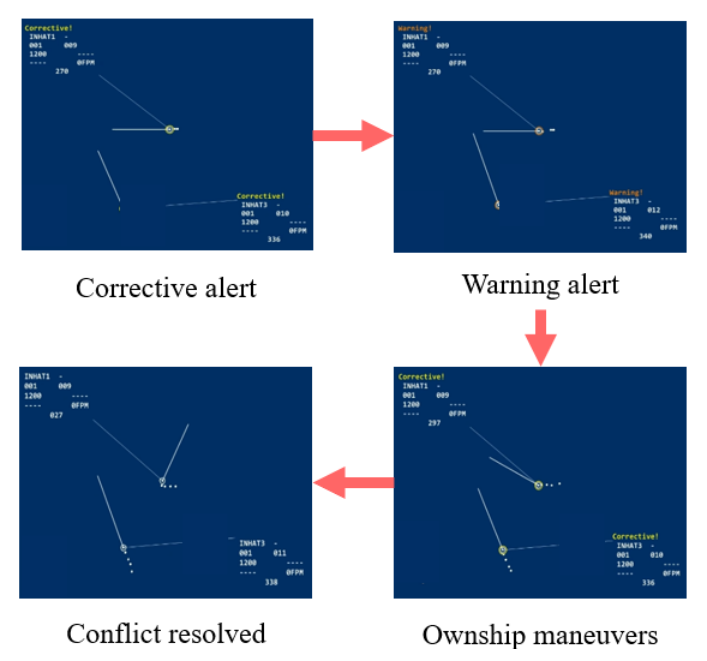


Fig. 19: UAS encounter scenario using Scaled DAIDALUS algorithm

#### V. CONCLUSIONS

This paper presents a hybrid HiTL simulation framework for evaluating DAA systems using small surrogate UASs. By scaling spatial parameters in proportion to the reduced speeds of the test vehicles, the timings of DAA alerts were preserved. Flight tests with ADS-B out-equipped drones demonstrated the feasibility of the system by replicating key alerting functionalities of full-scale DAA operations. These results confirm that the proposed approach can reduce the barriers associated with large-scale flight testings while maintaining fidelity in pilot-controller-DAA system interactions. Future studies are planned to include more complex multi-intruder scenarios with fixed wing surrogate UASs to analyze pilot-controller-DAA system interactions under demanding situations.

#### REFERENCES

- D. Kunertova, "Learning from the Ukrainian Battlefield Tomorrow's Drone Warfare, Today's Innovation Challenge," CSS Studies, August 2024.
- [2] R. Bridgelall, "Aircraft Innovation Trends Enabling Advanced Air Mobility," Inventions 2024, 9(4), 84.
- [3] A47-A11L.UAS.89 sUAS Mid-Air Collision (MAC) Likelihood Final Report, Alliance for System Safety of UAS through Research Excellence, February 2023.
- [4] DO-365A: Minimum operational performance standards (mops) for detect and avoid (data) system, RTCA Special Committee 228, 2020.
- [5] O. Shakernia, W. -Z. Chen, S. Graham, J. Zvanya, A. White, N. Weingarten, and V. Raska, "Sense and Avoid (SAA) Flight Test and Lessons Learned," AIAA Infotech@Aerospace 2007 Conference and Exhibit, Rohnert Park, California, USA, May 2007.
- [6] J. Pellebergs, "THE MIDCAS PROJECT," 27th CONGRESS OF THE INTERNATIONAL COUNCIL OF THE AERONAUTICAL SCI-ENCES, Nice, France, September 2010.
- [7] R. Arteaga, R. Kotcher, M. Cavalin, and M. Dandachy, "Application of an ADS-B Sense and Avoid Algorithm," 2016 AIAA Flight Testing Conference, Washington, D.C., U SA, Jun 2016.

- [8] Y. -C. Lai, and T. -Y. Lin, "Vision-Based Mid-Air Object Detection and Avoidance Approach for Small Unmanned Aerial Vehicles with Deep Learning and Risk Assessment," Remote Sensing, 2024, 16(5), 756.
- [9] D. H. Shim, and S. Sastry, "An Evasive Maneuvering Algorithm for UAVs in See-and-Avoid Situations," Proceedings of the 2007 American Control Conference, New York City, USA, July 2007.
- [10] E. De Lellis, E. Bove, U. Ciniglio, F. Corraro, G. Corraro, E. Filippone, N. Genito, and R. Palumbo, "Evaluating RPAS Integration with General Aviation Traffic by means of Real-Time Human-in-the-Loop Simulations," AIAA Scitech 2019 Forum, San Diego, California, USA, January 2019.
- [11] G. Corraro, F. Corraro, N. Genito, G. Di Capua, E. Filippone and C. Umberto, "Advanced Functions for Lowering Nuisance Alerts in a DAA System: Implementation and Performance Evaluation in Real-Time Human-in-the-Loop Testing," 2019 IEEE/AIAA 38th Digital Avionics Systems Conference (DASC), San Diego, CA, USA, September 2019.
- [12] Devin P. Jack, Keith D. Hoffler, Roy D. Roper, Anna Trujillo, Tod Lewis, Sagar KC and Dimitrios Tsakpinis, "Human-in-the-Loop Flight Simulation Experiment on Unmanned Aircraft Terminal Operations," AIAA Scitech 2020 Forum, Orlando, FL, USA, January 2020.
- [13] R. C. Rorie and L. Fern, "An Interoperability Concept for Detect and Avoid and Collision Avoidance Systems: Results from a Humanin-the-Loop Simulation," 2018 Aviation Technology, Integration, and Operations Conference, Atlanta, Georgia, USA, June 2018.
- [14] V. Di Vito and G. Torrano, "RPAS Automatic ADS-B Based Separation Assurance and Collision Avoidance System Real-Time Simulation Results," Drones, 2020, 4(4), 73.
- [15] C. Mu'noz, A. Narkawicz, G. Hagen, J. Upchurch, A. Dutle, M. Consiglio, and J. Chamberlain, "DAIDALUS: Detect and Avoid Alerting Logic for Unmanned Systems," in 2015 IEEE/AIAA 34th Digital Avionics Systems Conference (DASC), IEEE, September 2015, pp. 5A1-1-5A1-12
- [16] J. Park, J. Ryu, T. Kim, S. Lee, M. Park, and H. -T. Lee, "Overview of the Administrative Process of Using ADS-B out and Flight Test Results," Journal of Advanced Navigation Technology, 28(6): 844-854, Dec. 2024.